Microglial Response to Light-Induced Photoreceptor Degeneration in the Mouse Retina

Ana M. Santos, David Martín-Oliva, Rosa M. Ferrer-Martín, Mohamed Tassi, Ruth Calvente, Ana Sierra, Maria-Carmen Carrasco, José L. Marín-Teva, Julio Navascués, and Miguel A. Cuadros*
Departamento de Biología Celular, Facultad de Ciencias, Universidad de Granada, E-18071 Granada, Spain

ABSTRACT

The microglial response elicited by degeneration of retinal photoreceptor cells was characterized in BALB/c mice exposed to bright light for 7 hours and then kept in complete darkness for survival times ranging from 0 hours to 10 days. Photodegeneration resulted in extensive cell death in the retina, mainly in the outer nuclear layer (ONL), where the photoreceptor nuclei are located. Specific immunolabeling of microglial cells with anti-CD11b, anti-CD45, anti-F4/80, anti-SRA, and anti-CD68 antibodies revealed that microglial cells were activated in light-exposed retinas. They migrated to the ONL, changed their morphology, becoming rounded cells with short and thick processes, and, finally, showed immunophenotypic changes. Specifically, retinal microglia began to strongly express antigens recognized by anti-CD11b, anti-CD45, and anti-F4/80, coincident with cell degeneration. In contrast, upregulation of the antigen recognized by anti-SRA was not detected by immunocytochemistry until 6 hours after light exposure. Differences were also observed at 10 days after light exposure: CD11b, CD45, and F4/80 continued to be strongly expressed in retinal microglia, whereas the expression of CD68 and SRA had decreased to near-normal values. Therefore, microglia did not return to their original state after photodegeneration and continued to show a degree of activation. The accumulation of activated microglial cells in affected regions simultaneously with photoreceptor degeneration suggests that they play some role in photodegeneration. J. Comp. Neurol. 518:477–492, 2010.

INDEXING TERMS: microglia; photodegeneration; retina; cell death; immunocytochemistry

It is well known that light exposure induces retinal degeneration (Noell et al., 1966; Remé et al., 1998). Both bright light and continuous exposure to moderately intense light interfere with the visual cycle and induce photoreceptor death (Hao et al., 2002; Wenzel et al., 2005). It was recently demonstrated that cell death elicited by bright light exposure depends on rhodopsin bleaching, whereas the death induced by continuous exposure to light of moderate intensity requires phototransduction (Hao et al., 2002; Wenzel et al., 2005). Photoreceptor death is also an early event in the degeneration that takes place in the retina of animals with many types of inherited eye diseases, as observed in the different types of *rd* mice, in *rds* mice, in RCS rats, and in *rcd1* dogs, among others (Pierce, 2001). Although the altered genes differ in each of these animals, the common outcome is always a massive degeneration of photoreceptor cells (Pierce, 2001).

It has been classically considered that photoreceptors die by apoptosis in both inherited retinal degeneration and light-induced degeneration (Chang et al., 1993; Portera-Cailliau et al., 1994; Remé et al., 1998), although concerns have been raised on this issue (Lohr et al., 2006; Kunchithapautham and Rohrer, 2007; Sancho-Pelluz et al., 2008). The photoreceptor degeneration found in several human diseases, such as retinitis pigmentosa and age-related macular degeneration, show similar features to those observed in animals with inherited photoreceptor degeneration. Although the etiological factors involved would be different, retinal degeneration in these animals has frequently been used as a model of human retinal degenerations.

Microglial cells are considered to be cells of macrophage/monocyte lineage (Cuadros and Navascués, 1998) that continuously survey the nervous parenchyma in the normal adult central nervous system (CNS; Nimmerjahn et al., 2005). Their

Additional Supporting Information may be found in the online version of this article.

Grant sponsor: Spanish Ministry of Science and Innovation; Grant number: BFU2007-61659; Grant sponsor: Junta de Andalucía; Grant number: P07-CVI-03008.

*CORRESPONDENCE TO: Miguel A. Cuadros, Departamento de Biología Celular, Facultad de Ciencias, Universidad de Granada, E-18071 Granada, Spain. E-mail: macuadro@ugr.es

Received 16 July 2009; Revised 28 August 2009; Accepted 2 September 2009
DOI 10.1002/cne.22227
Published online September 16, 2009 in Wiley InterScience (www.interscience.wiley.com).

activation in response to CNS parenchyma alterations involves morphological, immunophenotypic, migratory, and proliferative changes (Kreutzberg, 1996; Davalos et al., 2005; Tambuyzer et al., 2009). It has been proposed that microglial activation is a graded response that depends on the cell environment and the nature and severity of the injury (Raivich et al., 1999; Lai and Todd, 2008) and can be either protective or toxic for neural cells (Polazzi and Contestabile, 2002; Hanisch and Kettenmann, 2007).

As in other parts of the CNS, microglial cells are also present in the normal retina, and their distribution through the retinal layers is well documented (Ashwell et al., 1989; Provis et al., 1996; Chen et al., 2002; Lee et al., 2008; Santos et al., 2008). Retinal microglia are activated in response to nearly all pathological states of the retina (Langmann, 2007), with microglial cells migrating to the layers affected by degeneration. Thus, the outer nuclear layer (ONL), which is devoid of microglial cells in normal retina (Santos et al., 2008), is colonized by these cells in conditions that induce massive ONL cell degeneration, such as inherited photoreceptor degeneration (Roque et al., 1996; Hughes et al., 2003; Zeng et al., 2005) and light (Ng and Streilein, 2001; Harada et al., 2002; Zhang et al., 2005) or laser (Lee et al., 2008) injury of the retina. Migration of microglial cells toward sites of degeneration has been also observed in other pathological situations (Rao et al., 2003; Marella and Chabry, 2004; García-Valenzuela et al., 2005; Lewis et al., 2005) and in pathological human retinas (Gupta et al., 2003). Besides migrating toward degenerating regions, activated microglial cells undergo immunophenotypic changes (Hughes et al., 2003; Langmann, 2007) and release products with either neurotrophic or neurotoxic action (Harada et al., 2002, Zeng et al., 2005; Zhang et al., 2005; Langmann, 2007; Sasahara et al., 2008).

This study analyzes in detail the migratory patterns and morphological and immunophenotypical changes of microglial cells after bright-light-induced photoreceptor degeneration, revealing that microglial cells respond quickly to photoreceptor degeneration and that some immunophenotypic changes persist 10 days after light exposure.

MATERIALS AND METHODS

Animals

Sixty adult BALB/c albino male mice of 60 days postnatal age (P60) provided by the Animal Facilities Service of the University of Granada were maintained in a normal 12-hour light/dark cycle before the start of experiments. Animals were killed by cervical dislocation at different time points after the light exposure (see below), because anesthesia may interfere with the effects of bright light on retinal photoreceptors (Keller et al., 2001; Remé et al., 2003). All experimental procedures followed the guidelines issued by the Research Ethics Committee of the University of Granada.

Induction of light damage

The response of microglia to retinal photoreceptor degeneration (photodegeneration) after bright light exposure was studied by exposing mice to bright light (Φ) and then keeping them in complete darkness for 0, 3, 6, 12, 18, 24, 36, 48, or 72 hours ($\Phi + 0$ hours, $\Phi + 3$ hours, $\Phi + 6$ hours, $\Phi + 12$ hours, $\Phi + 18$ hours, $\Phi + 24$ hours, $\Phi + 36$ hours, $\Phi + 48$ hours, and $\Phi + 72$ hours, respectively) or 10 days ($\Phi + 10$ days), as summarized in Figure 1. Several methods were employed to confirm that our light exposure procedure effectively produced photodegeneration.

Photic injury to mouse retinas was carried out as described by Grimm et al. (2000) with some modifications. Briefly, animals were dark-adapted for 20 hours before being exposed to bright light. Control group retinas were collected immediately after dark adaptation. The experimental mouse group was exposed for a further 7 hours to cool white light (Master PL Electronic 23W, 230-240V Cool Daylight, Royal Philips Electronics, Amsterdam, Holland) at a luminescence level of 10,000 lux, controlled by a luxometer (HD 9021, Delta Ohm SRL, Padua, Italy).

Histology

The entire enucleated eyes from control and light-exposed animals were fixed in periodate-lysine-paraformaldehyde (PLP; Yamato et al., 1984) for 6 hours at 4°C. Fixed material was cryoprotected in phosphate-buffered saline (PBS; 0.1 M, pH 7.4) containing 30% sucrose, soaked in OCT compound (Sakura Finitek Europe, Zoeterwoude, The Netherlands), and frozen in liquid nitrogen. Blocks were stored at −40°C until use. Transverse sections of 20-μm thickness were obtained in a cryostat (Leica, Wetzlar, Germany) and collected on SuperFrost slides (Menzel-Glasser, Braunschweig, Germany).

Antibody characterization and immunocytochemistry

The primary antibodies used in this study were all monoclonal antibodies produced in rat; their sources and dilutions are summarized in Table 1. Anti-F4/80 antibody was produced by taking spleen cells from a rat hyperimmunized with cultured thioglycollate-induced mouse peritoneal macrophages and fusing them with a mouse myeloma (Austyn and Gordon, 1981); it binds to a surface glycoprotein of about 160 kDa, as determined by immunoprecipitation and Western blot experiments (Austyn and Gordon, 1981 and manufacturer's technical information), present

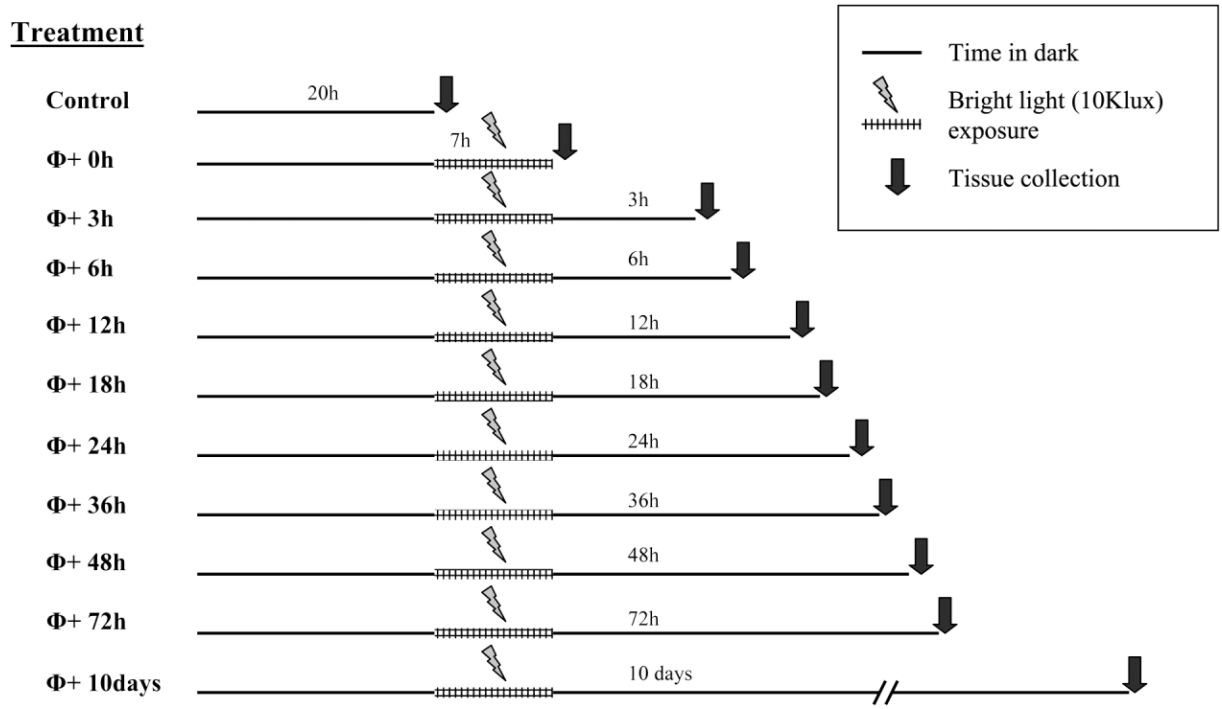

Figure 1. Schematic summary of the protocol used for analyzing bright light-induced degeneration (photodegeneration). Φ, bright light exposure.

TABLE 1.
Primary Antibodies Used in This Study

Antibody	Source, cat. no./clone	Dilution
Anti-F4/80	Serotec, Oxford, UKMCA497GA/CI:A3-1	1:200
Anti-CD45	Serotec MCA1388/IBL-3/16	1:40
Anti-CD68	Serotec MCA1957/FA-11	1:40
Anti-CD11b	Serotec MCA711G/5C6	1:100
Anti-SRA (CD204)	Serotec MCA1322/2F8	1:30

in mouse macrophages and microglia (Hume and Gordon, 1983; Perry et al., 1985).

Anti-CD45 and anti-CD68 antibodies recognize mouse homologues of CD45 and CD68 molecules, respectively. CD45 is a tyrosine phosphatase protein present in the membrane of cells of monocyte/macrophage lineage (Penninger et al., 2001). The antibody was generated by using purified B cells from mouse lymph nodes as immunogen (manufacturer's technical information); it recognizes a single band of >170 kDa in Western blot of mouse brain extracts (Cuadros et al., 2006).

The CD68 antigen, which is also known in mice as macrosialin, is a membrane glycoprotein present in lysosomes of macrophage-lineage cells (Da Silva and Gordon, 1999). The clone FA-11 was obtained by immunizing a rat with concanavalin A acceptor protein from the P815 cell line (manufacturer's technical information) and produces an antibody that recognizes, in Western blot, bands of 85–115 kDa specifically present in tissue macrophages that correspond to different degrees of glycosylation (Da Silva and Gordon, 1999).

Anti-CD11b binds to an integrin expressed on the surface of numerous leukocytes, including macrophages and microglial cells, and it is also known as macrophage-1 antigen (Mac-1) or complement receptor-3 (CR3). CD11b antigen participates in phagocytosis, chemotaxis, and cellular activation, among other processes (Solovjov et al., 2005) and was recently shown to be involved in microglial migration and cytotoxicity in pathological situations of the CNS (Pei et al., 2007; Wakselman et al., 2008). The antibody used was raised against mouse thioglycollate-elicited peritoneal macrophages and precipitates a heterodimer of 165 and 95 kDa (manufacturer's technical information). This antibody has been extensively used to label microglial cells (Dissing-Olesen et al., 2007)

Finally, the anti-SRA/CD204 antibody recognizes scavenger receptor class A (SRA; also known as scavenger receptor type I/II) in phagocytes and dendritic cells (Yamada et al., 1998). SRA, like all members of the scavenger family, plays an essential role in the innate immune response (Peiser et al., 2002; Block et al., 2007). In adult CNS, SRA is expressed on perivascular macrophages but

not on resting microglia (Mato et al., 1996). SRA expression increases in the CNS after LPS or kainic acid administration (Bell et al., 1994; Herber et al., 2006) and is considered a marker of microglial activation (Husemann et al., 2002; Alarcón et al., 2005; Block and Hong, 2005). Raw 264 cell line was used as immunogen to generate the antibody produced by the 2F8 clone (manufacturer's technical information) used in this study; it recognizes a band of around 90 kDa in peritoneal and resident macrophages under reducing conditions in immunoprecipitation and Western blot (Fraser et al., 1993; Daugherty et al., 2000).

As a negative control, primary antibodies were omitted in some sections, resulting in the absence of immunostaining. We also tested whether immunolabeled cells outside the retina showed the expected distribution and shape. Some cells appeared labeled within extraretinal tissues (blood vessels, vitreous, subretinal space, and periocular tissues) with anti-F4/80, anti-CD45, anti-CD68, and anti-CD11b as previously described (Kezic et al., 2008). Anti-SRA antibody labeling was observed in extraretinal tissues in some cells with the characteristics of macrophages (Yamada et al., 1998; Daugherty et al., 2000); in addition, SRA labeling was restricted to some cells related to blood vessels in control retinas, as described in other CNS regions (Husemann et al., 2002).

For immunostaining, sections were permeabilized in 0.1% Triton X-100 (Sigma, St. Louis, MO) in PBS (pH 7.4) and incubated with normal goat serum (Sigma) diluted 1:30 in PBS with 1% bovine serum albumin (PBS-BSA) for 45–60 minutes. They were then incubated with the primary antibody for 30–48 hours at 4°C, washed in PBS, and incubated with the secondary antibody diluted 1:500 in PBS-BSA for 2 hours at room temperature. The secondary antibody for all the primary antibodies was Alexa Fluor 488-conjugated goat anti-rat IgG (Molecular Probes, Eugene, OR). Finally, sections were stained with Hoechst 33342 (5 μg/ml in PBS, Sigma) for 2 minutes to label cell nuclei, washed, and coverslipped with Fluoromount G (Southern Biotech, Birmingham, AL).

Cell death assessment through quantification of cytoplasmic nucleosomes by ELISA

Cell death in normal and light-exposed retinas was quantified by using an enzyme-linked immunosorbent assay (ELISA) kit (Cell Death Detection ELISA, Roche Diagnostics, Mannheim, Germany), which contains a combination of antibodies that recognize histones and DNA, allowing quantification of soluble nucleosomes in retinal lysates. The two retinas from each animal were dissected in PBS and homogenized in 150 μl of protease inhibitor 1X (Complete Mini, EDTA-free, Roche Diagnostics, Munich, Germany) by using a Dounce homogenizer. Samples were then centrifuged at 13,200 rpm for 10 minutes at 4°C. After the pellet was discarded, the cytoplasmic nucleosome-containing supernatant (lysate) was stored at −40°C until use. A portion of the supernatant was used to quantify protein concentration by Bradford's method (Bio-Rad Protein Assay, Germany), and the rest was diluted 1:10 in the kit buffer and processed for ELISA following the manufacturer's protocol. Absorbance values were measured in a Multiskan Ascent (Thermo Fisher Scientific, Madrid, Spain) with a 405-nm filter. ELISA-obtained absorbance values (optical density [OD]) were referred to the protein concentration of each sample. The amount of cell death in control and light-exposed retinas was expressed as the mean OD value per μg of protein in each sample and represented in a histogram. Statistical significance was determined by using Student's t-test. Data were expressed as means ± SEM and obtained from at least three independent experiments for each time point.

In situ cell death detection by TUNEL

The localization of dead cells in the retina was investigated by using the terminal deoxynucleotidyl transferase (TDT)-mediated deoxyuridine triphosphate (dUTP) nick-end labeling (TUNEL) technique (Gavrieli et al., 1992). Sections from control and light-exposed retinas were washed in PBS, permeabilized in 0.1% Triton X-100 in PBS, and incubated in TDT buffer (Promega, Madison, WI; pH 6.8) containing 2% TDT (Promega) and 0.03% tetrametylrhodamine-dUTP (Roche Diagnostics) for 1 hour at 37°C. After incubation, sections were washed in PBS, stained with nuclear dye Hoechst 33342 (Sigma), and coverslipped by using Fluoromount G (Southern Biotech).

Transmission electron microscopy (TEM) analysis

Retinas from control and $\Phi + 6$ hours, $\Phi + 24$ hours, and $\Phi + 10$ days adult BALB/c mice were processed for TEM observation. The eyes were enucleated, and pieces of their posterior half were fixed in a mixture of 2% glutaraldehyde and 1% paraformaldehyde in 0.05 M cacodylate buffer (pH 7.4) supplemented with 2 mM Cl_2Mg for 3 hours. The retinas were postfixed in 1% osmium tetroxide in the same buffer for 1 hour, dehydrated in a graded series of ethanol, and embedded in Epon 812. Semithin sections (0.5 μm thick) were stained with toluidine blue, whereas ultrathin sections (50–70 nm) were mounted on copper grids and examined under a Zeiss EM10C electron microscope (Zeiss, Oberkochen, Germany).

Microscopy study and cell count

Semithin sections were observed under an AxioPhot microscope (Zeiss) equipped with an AxioCam digital camera (Zeiss). Confocal microscopy images of immunostained

sections were obtained by using a Leitz DMRB microscope equipped with a Leica TCS-SP5 scanning laser confocal imaging system (Leica). In confocal microscopy studies, stacks of horizontal (xy) optical sections of selected fields were collected at 0.5–1-μm intervals along the z-axis. Leica confocal software was used to superimpose optical sections from each microscopic field onto projection images. The images obtained by using normal or confocal microscopy were stored in TIFF format and prepared digitally by adjusting brightness, contrast, and evenness of illumination in Adobe Photoshop (Adobe Systems, San Jose, CA).

Microglial cells were counted in control and treated retinas in order to quantify the invasion of the outer retina (ONL and subretinal space) by activated microglial cells and macrophages after light exposure. Cell bodies displaying SRA immunoreactivity in the outer retina were counted in 20-μm-thick cryostat transverse retinal sections including both central and peripheral areas of the retina. Cells were only counted in every second section to avoid any double counting of SRA-positive cells. At least four retinas from different animals were counted at each survival time, and six sections were counted in each retina. Image J software (NIH, Bethesda, MD) was used to measure the ONL and subretinal space area in each section and estimate the density of SRA-positive cells (number of labeled cells per μm^2). Values (means ± SEM) were represented in a histogram and compared to establish statistical significance by using Student's t-test.

RESULTS

Assessment of retinal damage after light exposure

Several methods were employed to confirm that the light exposure procedure used in this study was effective in producing photodegeneration. Semithin sections showed that retinas subjected to the photodegeneration protocol were thinner than control ones (Fig. 2A). The retinal thinning was mainly due to the decrease in size of the ONL as a consequence of a fall in the number of photoreceptors. Pyknotic nuclei were frequently seen in semithin sections of light-exposed retinas but were scarce in normal retinas. These observations indicated the death of numerous photoreceptors.

TEM studies revealed disorganization of the arrangement of the nuclei in the ONL and the presence of degenerating photoreceptor cells in light-treated retinas shortly after the light exposure (Fig. 2B–D). The observation of different morphological features in degenerating nuclei suggested that photoreceptors can degenerate in more than one way (compare the nuclei indicated by arrows in Fig. 2C,D). TEM also showed numerous degenerated photoreceptor outer segments and hypertrophied cells of the retinal pigment epithelium, containing abundant inclusions (Supplementary Figure 1).

Retinal cell degeneration was quantified by using an ELISA to determine the number of free nucleosomes in retinal extracts, revealing that cell death increased significantly after light exposure (Fig. 3A). The number of free nucleosomes remained elevated until $\Phi + 48$ hours and decreased thereafter, although cell death continued to be higher in $\Phi + 10$ days retinas than in control ones.

The TUNEL technique was used to determine the localization of degenerating cells within the retina. TUNEL-labeled nuclei were not detected in control retinas (Fig. 3B) but were observed in $\Phi + 6$ hours retinas and became more numerous from $\Phi + 24$ hours on (Fig. 3C). Most degenerating nuclei were in the ONL (Fig. 3C–E), where photoreceptor cell nuclei were located, although some TUNEL-labeled nuclei also appeared in the inner nuclear layer (INL) in $\Phi + 36$ hours (Fig. 3D) and $\Phi + 48$ hours retinas (not shown).

Therefore, observations using different methods gave comparable results and showed significantly greater cell death in the ONL of light-treated versus control retinas.

Microglial response in light-damaged retinas

As previously reported (Lee et al., 2008; Santos et al., 2008), microglial cells in the normal mature mouse retina bore numerous thin processes that were profusely ramified (Fig. 4A) and located in the ganglion cell layer (GCL), inner plexiform layer (IPL), INL, and outer plexiform layer (OPL).

The distribution pattern of microglial cells in the retinal layers differed between light-exposed and control retinas. After light exposure, numerous labeled cells invaded the ONL, which was devoid of them in normal retinas. Abundant large macrophages appeared in the subretinal space from $\Phi + 0$ hours on (Fig. 4B,C), contrasting with the lower number and the smaller size of these cells in normal eyes (Fig. 4A). TEM observations also revealed the presence of infiltrated cells in the ONL and subretinal space of light-exposed retinas (Fig. 2D,E). In the light microscopy study, similar cells were immunolabeled with macrophage/microglial markers. Immunolabeled cells in the subretinal space had an ameboid shape, with no processes or bearing one or two short thick processes. Some cells in this localization contained phagosomes, apparently including debris from degenerating outer segments of photoreceptor cells (Figs. 2E, 4C).

Our observations suggested that most immunolabeled cells in the ONL came from the retina itself, at least at short survival times. Hence, they were considered to be microglial cells. In fact, labeled cells (or labeled cell processes) were already present in the ONL at $\Phi + 0$ hours, appar-

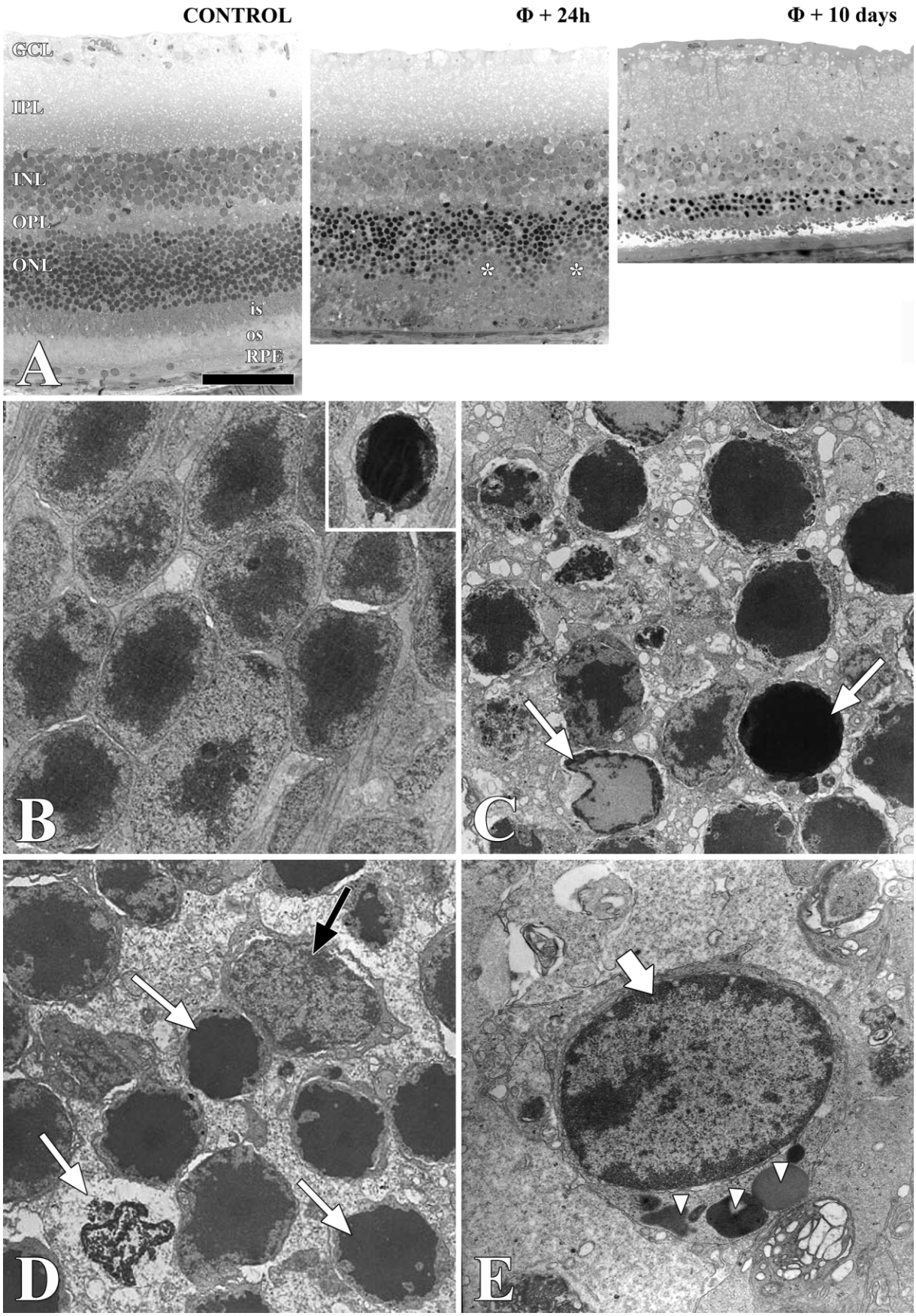

Figure 2

ently coming from microglial cells in other layers of the retina (Fig. 4B).

Figure 4 summarizes the morphological changes in retinal microglial cells invading the ONL after light exposure (Fig. 4D–G). From Φ + 6 hours on, some microglial cells became larger and with thicker processes than in control retinas; some of these processes were directed toward the ONL (Fig. 4D). Afterward, the processes of microglial cells were more deeply introduced in the ONL, where they simultaneously engulfed several photoreceptor cells (Fig. 4E). Finally, microglial cells appeared entirely within the ONL, always engulfing several photoreceptor somas (Fig. 4F) and showing a honeycomb appearance (Fig. 4G). The supplementary video offers additional evidence of the close association between degenerating photoreceptors and honeycomb-like microglial cells.

Immunophenotypical changes in macrophage/microglial cells in light-damaged retinas

A panel of microglial markers was used to obtain a more accurate account of the microglial response in bright-light-damaged retinas, and following changes in their expression after photodegeneration. Specifically, we studied the labeling pattern of the molecules recognized by anti-CD11b, anti-CD45, anti-F4/80, anti-SRA, and anti-CD68 antibodies. In general, the distribution pattern of cells labeled with these markers showed significant differences between control and light-exposed retinas, although not all markers yielded the same staining pattern, as reported below.

Anti-CD11b immunolabeling revealed the normal distribution of microglial cells in the adult control retinas, showing ramified microglial cells in the GCL, IPL, INL, and OPL (Figs. 4A, 5A). In Φ + 0 hours retinas, CD11b-positive cells

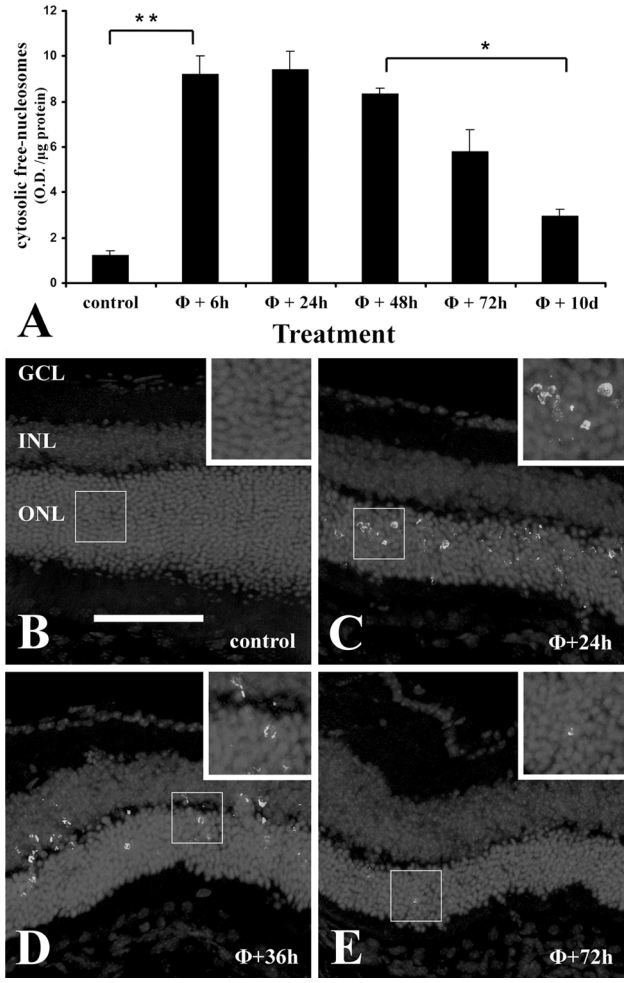

Figure 3. Cell death in light-exposed retinas. **A:** Quantification of free cytosolic nucleosomes by ELISA in light-exposed retinas. The amount of free nucleosomes (sign of cell death) is higher at Φ + 6 hours, remained elevated for nearly 3 days, and then decreased. Data are expressed as mean ± SEM of three independent experiments. Asterisks denote significant differences between the indicated values (*, $P < 0.05$; ** $P < 0.01$). B–E: TUNEL staining reveals the presence of cell death fragments in the different retinal layers (shown by Hoechst staining of nuclei). **B:** No TUNEL-labeled structures are found in control retinas. **C:** Retinas from light-exposed animals contain frequent TUNEL-positive bodies in the ONL, which become more abundant from Φ + 24 hours onward. **D:** At Φ + 36 hours, TUNEL labeling is also seen in the INL. **E:** From Φ + 48 hours onward, TUNEL labeling is again decreased, and very few TUNEL-positive bodies are seen 72 hours after light exposure O.D., optical density; GCL, ganglion cell layer; INL, inner nuclear layer; ONL, outer nuclear layer. Inserts in B–D show a twofold magnification of the boxed area in each image. Scale bar in B = 60 µm in B; 97 µm for C; 75 µm for D,E.

Figure 2. Analysis of retinal damage after light exposure. Light and electron micrographs are taken from the central region of mouse retinas. **A:** Semithin sections of control and light-exposed retinas stained with toluidine blue. In control retinas (left panel), well-ordered photoreceptor inner (is) and outer (os) segments can be seen, whereas the outer nuclear layer (ONL) shows more than 10 rows of photoreceptor nuclei. One day after light exposure (Φ + 24 hours, center panel), the inner and outer segments are disorganized (asterisks), and numerous pyknotic nuclei appear in the ONL. Note that the ONL becomes thinner over time. At 10 days after light exposure (Φ + 10 days, right panel), photoreceptor cell loss is evident, with a reduction in ONL thickness in some regions to two to three rows of photoreceptor nuclei. B–E: Transmission electron microscopy (TEM) images of the ONL and the subretinal space. **B:** TEM micrograph of a control ONL, in which photoreceptor nuclei are regularly arranged. Isolated pyknotic nuclei are sometimes observed (insert). **C,D:** TEM micrographs of treated retinas obtained 6 and 24 hours after light exposure, respectively. The ONL is clearly disorganized, with numerous degenerating nuclei with different morphologies (white arrows). The presence of infiltrated cells is frequent in this layer (black arrow in D). **E:** Infiltrated cell (arrow) in the subretinal space of a treated retina, showing several phagosomes (arrowheads) in the cytoplasm. GCL, ganglion cell layer; IPL, inner plexiform layer; INL, inner nuclear layer; OPL, outer plexiform layer; ONL, outer nuclear layer; is, photoreceptor inner segments; os, photoreceptor outer segments; RPE, retinal pigment epithelium; Φ, bright-light exposure. Scale bar in A = 50 µm in A; 3.4 µm for B–D; 1.6 µm for E

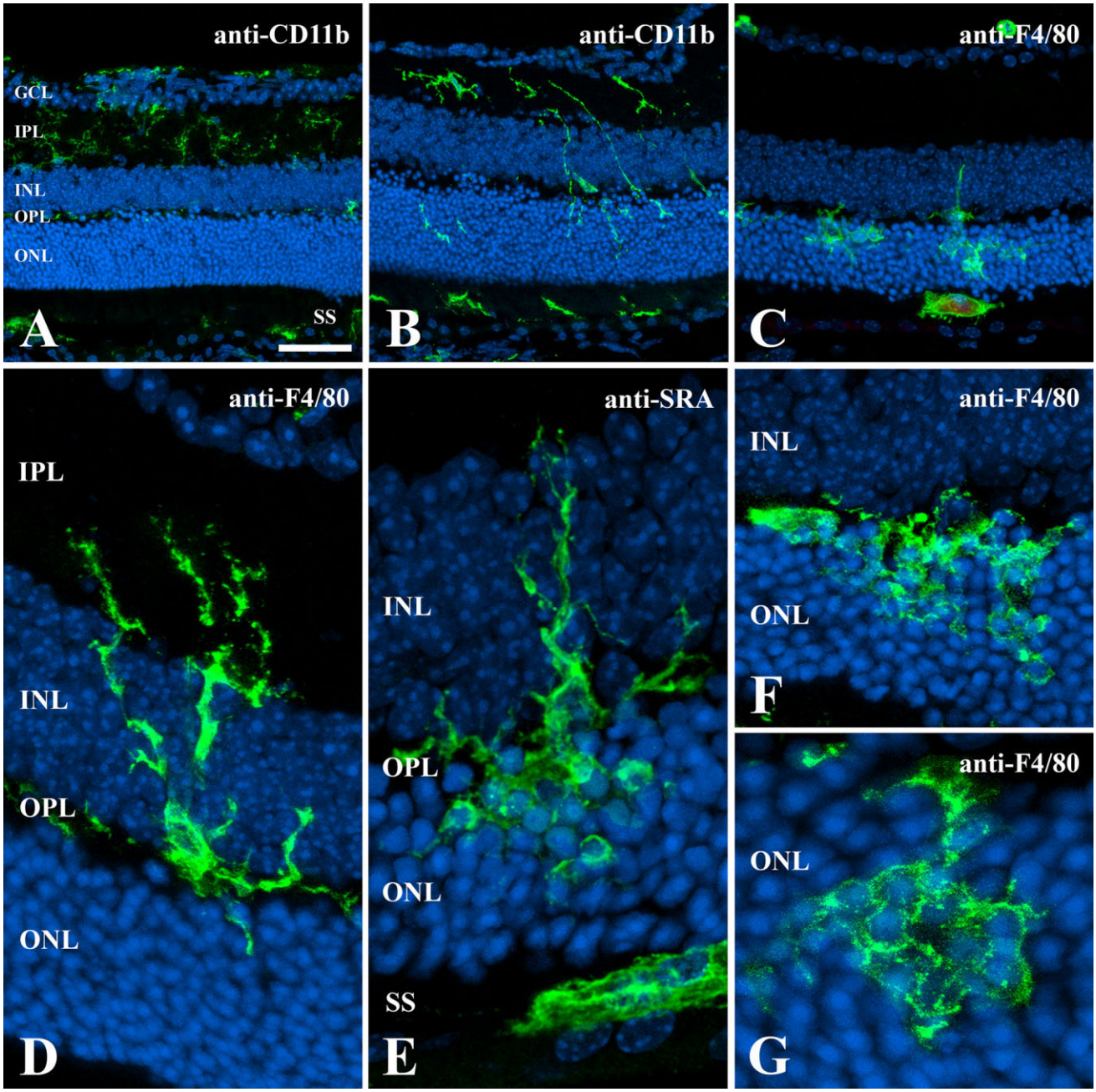

Figure 4. Changes in microglia distribution pattern and morphology after photodegeneration, as shown by immunolabeling with different microglial markers (green). Confocal microscopy. Hoechst (blue) was used to label cell nuclei. **A:** Distribution of CD11b-positive microglia in a control BALB/c adult retina. Microglial cells are present in the GCL, IPL, and OPL, but not in the INL or ONL. **B:** In $\Phi + 0$ hour retinas, CD11b-positive cells invade the ONL by extending long processes toward the ONL, the lesion site. The number and size of macrophages in the subretinal space is also increased. **C:** Two days after light exposure ($\Phi + 48$ hours), F4/80-positive microglial cells have completely invaded the ONL, simultaneously engulfing several photoreceptor somas. In the subretinal space, the presence of large macrophages is very frequent, and many contain phagosomes packed with pigment debris (red autofluorescence) from degenerating outer segments of photoreceptor cells. **D–G:** Morphological changes in microglial cells after photodegeneration. Highly ramified microglia in the plexiform layers of control retinas become large cells with short and thick processes after activation in response to photoreceptor degeneration. They invade the ONL and engulf several photoreceptor somas, acquiring a honeycomb appearance (D, $\Phi + 36$ hours retina; E, $\Phi + 48$ hours retina; F, $\Phi + 24$ hours retina; G, $\Phi + 12$ hours retina). GCL, ganglion cell layer; IPL, inner plexiform layer; INL, inner nuclear layer; OPL, outer plexiform layer; ONL, outer nuclear layer; SS, subretinal space. Scale bar in A = 50 μm in A and for B; 35 μm for C; 24 μm for D; 10 μm for E; 14 μm for F; 7 μm for G.

were observed apparently crossing the retina toward the ONL (Fig. 4B) in response to photodegeneration. In Φ + 12 hours retinas, CD11b-positive cells were mainly located in the ONL, whereas they were scarce in the other retinal layers (Fig. 5B), suggesting that microglial cells moved from the inner to the outer layers of the retina. Large macrophages were also labeled in the subretinal space. In Φ + 72 hours retinas; CD11b-positive ramified microglial cells were again observed in the inner layers of the retina and were still present in Φ + 10 days retinas (Fig. 5C).

Anti-CD45 antibody also labeled microglial cells in the GCL, IPL, INL, and OPL of control retinas (Fig. 5D). The intensity of anti-CD45 labeling was increased in light-exposed retinas, and strongly marked cells appeared in the ONL (Fig. 5E). In general, the distribution pattern of CD45-positive cells was similar to that described for CD11b-labeled cells at the different survival times after light exposure (Fig. 5E,F). The scleral border of the ONL showed hollows in association with large CD45-positive cells (Fig 5E). These hollows were seen from Φ + 6 hours to Φ + 48 hours.

Very few microglial profiles were weakly labeled with anti-F4/80 in control retinas, whereas strong labeling was seen in some cells of the subretinal space (Fig. 5G). In contrast, numerous F4/80-positive cells were seen across the different layers of light-treated retinas (Fig. 5H,I). As observed in CD45-labeled retinas, large F4/80-positive cells occupied the hollows in the scleral border of the ONL (Fig. 5H) and frequently contained autofluorescent phagosomes.

Control retinas were nearly devoid of anti-SRA labeling (Fig. 5J), which only marked scarce cells associated with blood vessels. Increased SRA expression was observed at Φ + 6 hours (not shown), although it was more patent afterward (Fig. 5K). At Φ + 10 days, anti-SRA labeling had almost completely disappeared in the retina (Fig. 5L).

Anti-CD68 labeling was seldom observed in control retinas (Fig. 5M). The intensity of labeling was higher across the retinal layers until day 3 after light exposure (Fig. 5N) but decreased thereafter (Fig. 5O). Unlike the above-mentioned cell membrane markers, which labeled highly complex cells with developed processes, anti-CD68 labeling was mostly restricted to lysosomal membranes in non-activated cells. Therefore, the CD68 labeling, which was dotted in less activated microglial cells (Fig. 6A), filled the entire cytoplasm of more activated cells in the ONL, such as the honeycomb-like microglia (Fig. 6B).

In Φ + 10day retinas, microglial cells continued to be intensely labeled with anti-CD11b, anti-CD45 and anti-F4/80 antibodies but anti-CD68 and anti-SRA labeling had returned to normal levels, and few cells were labeled with either marker in the retina (compare C, F, and I with L and O in Fig. 5).

Quantitative analysis of infiltrating macrophage/microglial cells in the ONL and subretinal space

The presence of activated microglia in the ONL and subretinal space was studied by recording the number of SRA-labeled cells. SRA antibody labeling was selected for the cell count because it reliably distinguished between resting and activated cells. Scarce SRA-positive cells were seen in the subretinal space of control retinas (Fig. 7) whereas their density in the ONL and subretinal space significantly increased from Φ + 6 hours to Φ + 48 hours and decreased thereafter (Fig. 7). In fact, SRA-positive cells were significantly less numerous in Φ + 72 hours retinas than at previous stages, and their density in Φ + 10 days retinas reached a value close to that in control retinas (Fig. 7).

Morphological evidence of the entry of microglial precursors into light-exposed retinas

Interestingly, at Φ + 18 hours, Φ + 24 hours, and Φ + 36 hours, cells immunolabeled with anti-CD11b (Fig. 5B), anti-F4/80 (Fig. 5H), and anti-SRA (Fig. 5K) antibodies were frequently observed on the vitreal surface of the retina, apparently crossing the retinal border (Fig. 8A,B) and ramifying within the IPL. This process appeared to be delayed in marginal regions of the retina (Fig. 8C).

DISCUSSION

Macrophage/microglial cells migrate toward the ONL after retinal photoreceptor degeneration in different experimental models (Thanos, 1992; Roque et al., 1996; Harada et al., 2002; Gupta et al., 2003; Hughes et al., 2003; Zeiss and Johnson, 2004; Zeiss et al., 2004; Zeng et al., 2005; Zhang et al., 2005; Joly et al., 2009). The present study investigated the time course of the macrophage/microglial response elicited by photodegeneration, analyzing immunolabeled retinas collected at different survival times after light exposure.

Different techniques were used to verify extensive degeneration of the light-treated retinas, which was mainly restricted to the ONL. Morphological features varied among the atypical nuclei of degenerating photoreceptors, suggesting that not all of them degenerate by apoptosis, as previously reported (Portera-Cailliau et al., 1994; Remé et al., 1998).

Results obtained demonstrated that microglial cells activate in the retina after photodegeneration induced by exposure to bright light. The ONL, which contained most of the degenerating cell nuclei observed, was invaded by microglial cells immediately after the light exposure period (Φ + 0 hours; see Fig. 4B). Because microglial cells are not

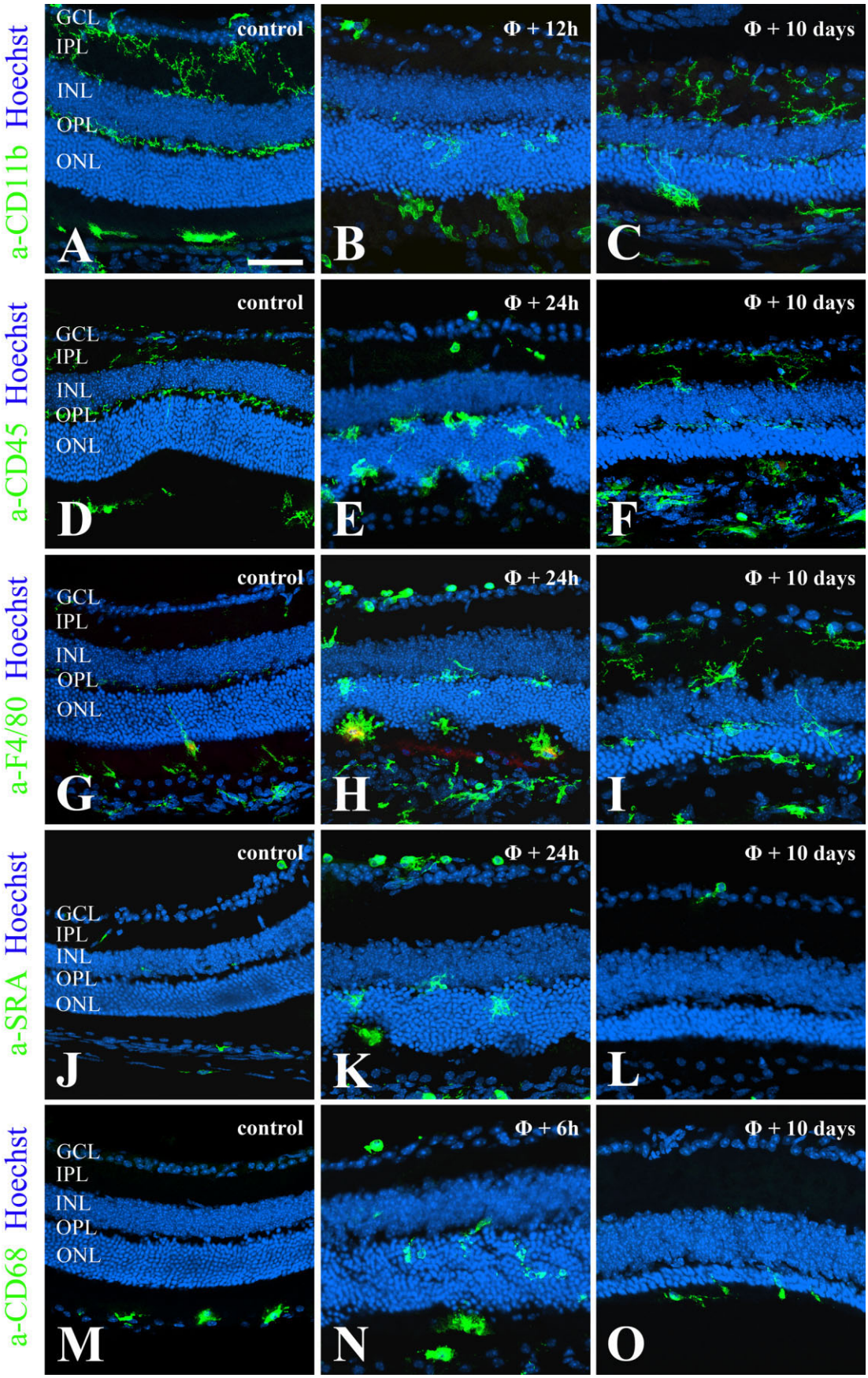
a-CD11b Hoechst
a-CD45 Hoechst
a-F4/80 Hoechst
a-SRA Hoechst
a-CD68 Hoechst
GCL
IPL
INL
OPL
ONL
control
Φ + 12h
Φ + 10 days
Φ + 24h
Φ + 6h
A
B
C
D
E
F
G
H
I
J
K
L
M
N
O

Figure 5

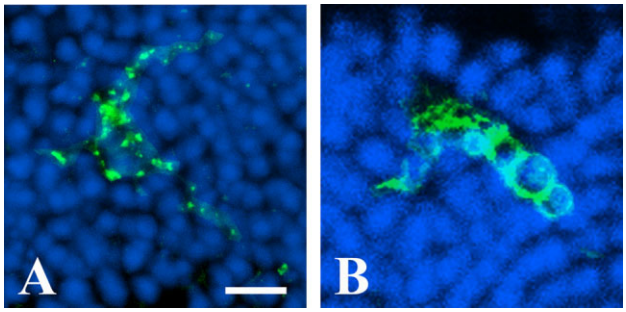

Figure 6. Changes in the expression pattern of the lysosomic marker anti-CD68 after light exposure. Confocal microscopy. Hoechst staining (blue) was used to reveal retinal layers. Anti-CD68 labeling (green) is mostly restricted to lysosomal membranes, showing punctuate staining in weakly activated microglial cells (**A**, ONL of a $\Phi + 3$ hours retina), whereas it covers the entire cell in more activated microglia (**B**, ONL of a $\Phi + 48$ hours retina). Scale bar in A = 8 μm in A; 7 μm for B.

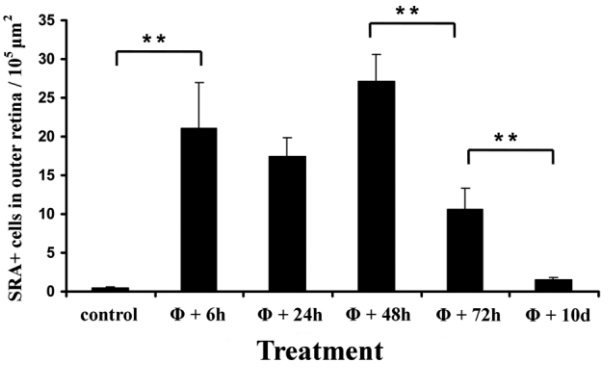

Figure 7. Quantitative analysis of SRA-positive macrophage/microglial cells infiltrating the ONL and subretinal space after light exposure. In control retinas, the outer retina contains few SRA-positive cells. However, a significant increase in the density of SRA-positive cells in the outer retina is observed from $\Phi + 6$ hours and maintained for 2 days, decreasing from $\Phi + 72$ hours and returning to almost normal levels at 10 days post light exposure. Data are expressed as mean ± SEM of three independent experiments (**, $P < 0.01$).

present in this layer in normal retinas (Santos et al., 2008), they should invade the ONL from inner regions of the retina, as suggested by our observations (Fig. 9). It is noteworthy that CD11b-positive microglial cells disappeared from the inner retina coincidentally with the microglial invasion of the ONL, implying that microglial cells in this layer mostly come from the IPL and INL. Moreover, microglial cells in the IPL and INL of anti-CD11b immunolabeled $\Phi + 0$ hours and $\Phi + 3$ hours retinas showed cellular processes oriented toward the ONL. A similar migration of microglial cells within the degenerating retina was demonstrated in other experimental models. Thus, studies of RCS rats (Thanos, 1992) and mice exposed to continuous light (Ng and Streilein (2001) found that microglial cells, which had phagocytosed labeled ganglion cell debris in the inner retina, migrated to the ONL and subretinal space.

Figure 5. Time course of microglial marker expression and morphology in control and light-exposed retinas. Each row shows representative micrographs obtained by confocal microscopy of control and light-exposed retinas at the time indicated in the upper right corner of the panel with the antibodies listed on the left: anti-CD11b (a-CD11b, **A–C**); anti-CD45 (a-CD45, **D–F**); anti-F4/80 (a-F4/80, **G–I**); anti-SRA (a-SRA, **J–L**), and anti-CD68 (a-CD68, **M–O**). Antibody labeling appears in green, and Hoechst staining (blue) was used to reveal the retinal layers. "Resting" microglia are seen in control retinas (first column) expressing CD11b (A) and CD45 (D) whereas virtually no microglial cells are labeled with anti-F4/80 (G), anti-SRA (J), or anti-CD68 (M). From 6 to 24 hours after light exposure (second column), labeled cells have invaded the ONL, showing shorter and thicker processes and increased levels of all five markers. At 10 days after light exposure (third column), SRA (L) and CD68 (O) expression has returned to control levels whereas CD11b (C), CD45 (F), and F4/80 (I) remain elevated and are expressed on both round and ramified cells. GCL, ganglion cell layer; IPL, inner plexiform layer; INL, inner nuclear layer; OPL, outer plexiform layer; ONL, outer nuclear layer. Scale bar in A = 45 μm in A; 40 μm for B,F,K,L; 35 μm for C,I,N,O; 50 μm for D,E,G,H,J,M.

Our results show that ramified microglia were almost absent from the GCL, IPL, and INL at early survival times after light exposure (until $\Phi + 48$ hours) but were again observed in these retinal layers from $\Phi + 72$ hours. It can be assumed from these observations that further microglia arrive in these layers between $\Phi + 48$ hours and $\Phi + 72$ hours. Two possible origins for these microglia can be envisaged. First, microglial cells may return to the GCL, IPL, and INL after fulfilling their role in the ONL; however, this is unlikely because numerous microglial cells were still seen in the ONL at times when they were again present in the inner layers of the retina. Second, new microglial cells may be incorporated after migrating from outside the retina, such as the vitreous body, choroid, ciliary body, or other CNS regions via the optic nerve. In fact, we frequently observed cells labeled with anti-CD45, anti-SRA, or anti-CD11b apparently entering the retina from the vitreous (Fig. 8). A recent paper (Joly et al., 2009) describes the incorporation of blood-borne macrophages into the injured retina via the optic nerve and ciliary body. Furthermore, entry of microglial cells into the retina from the vitreous and ciliary body during development has been described in mammals (Diaz-Araya et al., 1995; McMenamin, 1999; Santos et al., 2008) and birds (Marín-Teva et al., 1999). Our observations support the entry of an appreciable number of new microglial cells into the retina from the vitreous after photodegeneration, but we cannot rule out the entry of some microglial cells from other CNS regions or the choroid.

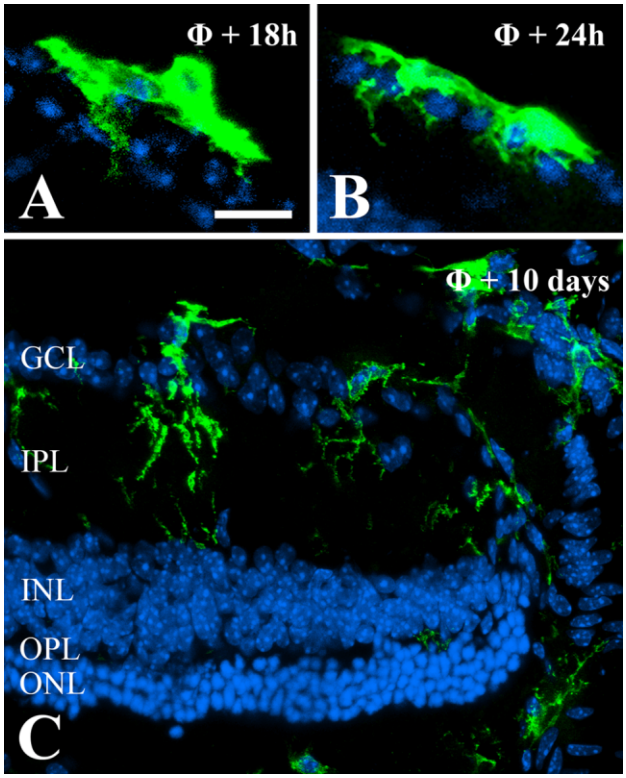

Figure 8. Entry of microglial precursors into the retina after photodegeneration. **A,B:** SRA-positive cells in the vitreal border with processes apparently traversing the GCL (light-treated retinas at 18 and 24 hours, respectively). **C:** At 10 days after light exposure, CD45-positive ramified cells were frequently seen in the peripheral region of the retina, apparently traversing the GCL to enter the retinal parenchyma. Confocal micrographs were obtained, and Hoechst staining (blue) was used to reveal retinal layers. GCL, ganglion cell layer; IPL, inner plexiform layer; INL, inner nuclear layer; OPL, outer plexiform layer; ONL, outer nuclear layer; Φ, bright-light exposure. Scale bar in A = 17 μm in A; 15 μm for B; 25 μm for C.

It is also possible that part of the increase in microglial cells in the retina results from local proliferation. However, we detected no microglial cells labeled with the proliferation marker anti-Ki67 (not shown) and no mitotic microglia were observed. New experiments are required to confirm that the proliferation is not a part of the microglial response elicited by photodegeneration. In this respect, several studies have shown that local proliferation of microglial cells is not always a component of microglial activation (Rogove et al., 2002; Gowing et al., 2008), and reduced proliferation of microglial cells has been observed in hypoxia-induced retinal lesions (Davies et al., 2006) and in a mouse model of glaucoma (Inman and Horner, 2007).

Our study also shows that microglial cells undergo immunophenotypical changes in response to photodegeneration. Labeling with all studied markers was much more intense in microglial cells invading the ONL than in control cells, although the most evident change was observed with the anti-SRA antibody. SRA immunolabeling was scarce in normal retinas and became abundant after photodegeneration. Immunophenotypical changes of some markers were already observable immediately after light exposure (Φ + 0 hours) and became more evident at subsequent survival times. Ten days after photodegeneration, the expression of CD68 and SRA had almost returned to control levels, whereas F4/80, CD11b, and CD45 labeling continued to increase.

SRA is a member of the scavenger receptor family, which can be expressed in microglial cells (Husemann et al., 2002; Block and Hong, 2005). SRA appears in microglial cells of the mouse brain during development but is downregulated in parenchymal microglia of the normal adult brain, although it continues to be present in perivascular macrophages (Mato et al., 1996). However, strong SRA expression is observed in microglial cells in the pathological CNS (Bell et al., 1994; Husemann et al., 2002; Herber et al., 2006), where it participates both in the interaction of phagocytic cells with host cells and in the phagocytosis of apoptotic cells (Platt and Gordon, 2001; Husemann et al., 2002). In line with findings in the hippocampus (Herber et al., 2006), our study shows that SRA expression in microglial cells is transient, appearing later than other microglial markers and absent at Φ + 10 days. The increase in SRA expression may be related to: migration of microglial cells toward degeneration regions, recognition of dead (or dying) cells, and/or an increase in the phagocytic

Figure 9. Schematic representation of microglial response to bright light-induced photodegeneration in the BALB/c mouse retina as assumed from observations in this study. Nuclear and plexiform layers appear in blue and yellow, respectively, whereas macrophage and microglial cells are in red. **A:** In the control retina, highly ramified microglial cells are mainly located in the GCL, IPL, and OPL whereas macrophages in the subretinal space (SS) are scarce and small in size. **B:** Immediately after light exposure (Φ + 0 hours), the microglial distribution changes, and cells located in the GCL, IPL, and OPL emit processes toward the ONL. Macrophages in the SS and outer segments (OS) become abundant and larger. **C:** In Φ + 24 hours retinas, microglial cells are virtually absent from the inner layers of the retina, suggesting a radial migration toward the injured ONL, which is entirely invaded by microglial cells. Many of these engulf several photoreceptors, acquiring a honeycomb appearance. Macrophages in the SS are frequently located in hollows that appear on the scleral border of the ONL as a consequence of photodegeneration. Numerous microglial precursors accumulate on the vitreal border of the retina, and some of them are apparently crossing the GCL to enter the retinal parenchyma. **D:** Ramified microglial cells replenish the empty inner layers (GCL and IPL) of the retina from Φ + 72 hours onward and show a more activated phenotype than in control retinas, with many processes invading the INL and ONL. Macrophages in the SS, which frequently introduce thin processes into the reduced ONL, remain numerous and large in size. VIT, vitreous; NFL, nerve fiber layer; GCL, ganglion cell layer; IPL, inner plexiform layer; INL, inner nuclear layer; OPL, outer plexiform layer; ONL, outer nuclear layer; OS, outer segments of photoreceptor cells; SS, subretinal space; PE, pigment epithelium; Φ, bright light exposure.

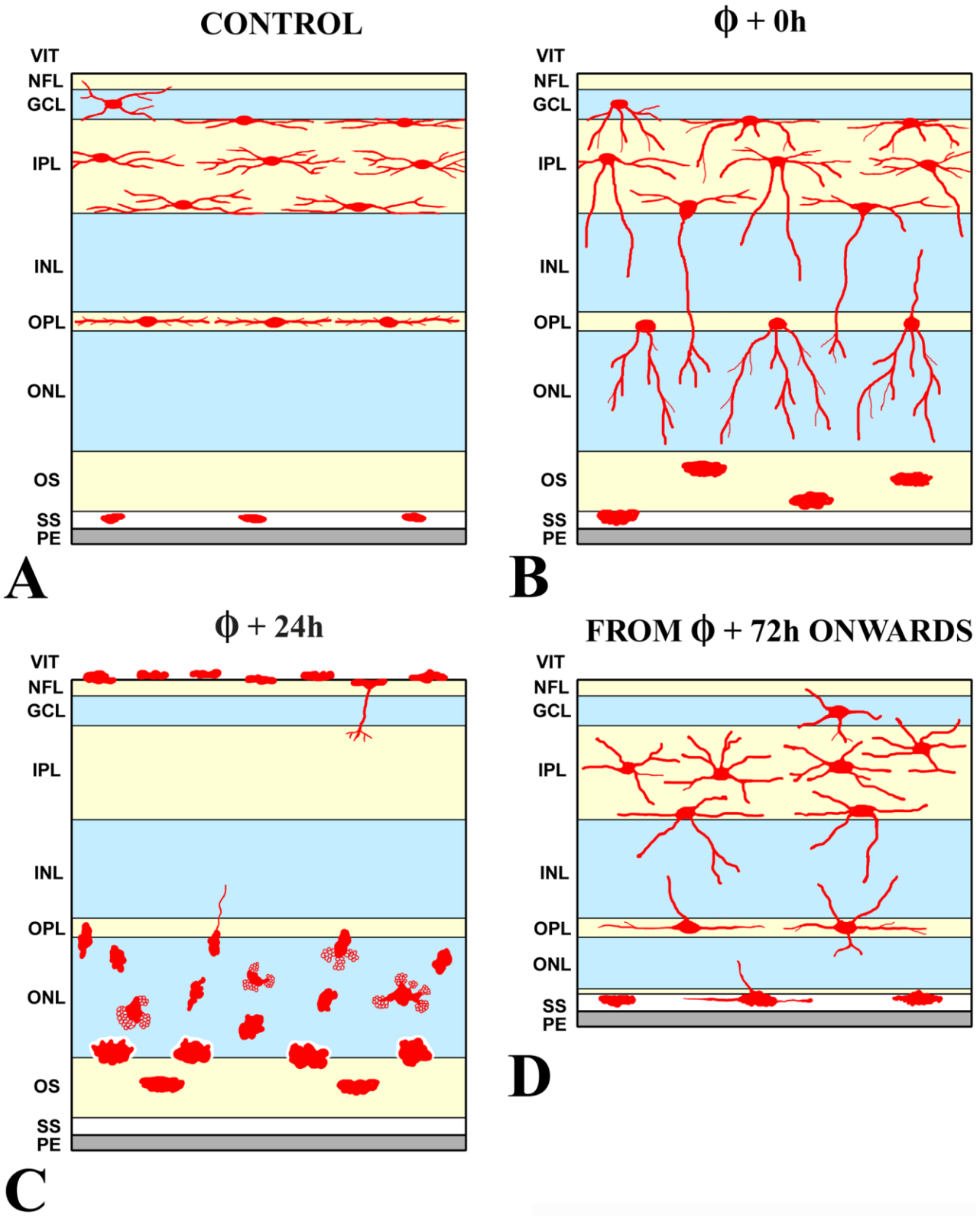

Figure 9

ability of microglia. Therefore, SRA expression would be increased when signals from degenerating cells begin to operate and would disappear when cell death has ended.

The lysosomal marker CD68 (macrosialin in mice) is a glycoprotein present in the lysosomes and plasma membrane of cells of monocyte lineage (Kurushima et al.,

2000). It has been related to cell adhesion and internalization of bound ligands (Kurushima et al., 2000) and may also be involved in the phagocytic activity of microglia in the degenerating retina. As with SRA, the expression of CD68 increased at around $\Phi + 6$ hours and was downregulated in microglial cells by $\Phi + 10$ days, suggesting that the expression of these two markers may be related to similar factors.

In contrast to SRA and CD68 immunolabeling, microglial cells labeled with anti-F4/80, anti-CD4, and anti-CD11b antibodies were detected before $\Phi + 6$ hours and continued to be robustly labeled at $\Phi + 10$ days. A similar nonsynchronic expression of different microglial markers was described in the mouse hippocampus after intracerebral injection of LPS (Herber et al., 2006). Taken together, our results show that retinal microglia at 10 days after light exposure are morphologically similar to ramified microglial cells in control retinas but are immunophenotypically different, suggesting the persistence of a certain degree of activation.

The role of microglial cells in neurodegeneration remains controversial (Lalancette-Hébert et al., 2007; El Khoury and Luster, 2008). In our photodegeneration model, activated microglial cells are seen in close contact with several photoreceptor somas (Fig. 4D–G), acquiring a honeycomb appearance. However, the functional significance of these contacts has not yet been elucidated. They could promote either photoreceptor cell death or photoreceptor survival. In support of the former, TEM observations show close association between infiltrated cells in the ONL and degenerating photoreceptors (Fig. 2D), and microglial activation occurs simultaneously with photoreceptor degeneration in our model. It should also be noted that microglial cells may have "distant" effects on photoreceptors by releasing cytokines and other soluble bioactive molecules that can promote the survival (Harada et al., 2002) or degeneration of photoreceptors (Zeng et al., 2005; Zhang et al., 2005; Langmann, 2007).

The final outcome of microglial activation would depend on the type of effect that predominates in each case (Hanisch and Kettenmann, 2007; Biber et al., 2007; Langmann, 2007).One of the possible beneficial effects of microglia is the phagocytosis of cell debris, whose accumulation can elicit an inflammatory reaction. Our TEM findings corroborated the phagocytic activity of the microglia, revealing frequent phagocytic inclusions in the cytoplasm of the microglial cells that entered the ONL. In addition, some microglial cells contained red autofluorescent bodies, which apparently correspond to phagosomes loaded with pigment debris from degenerated photoreceptors, as previously reported (Kezic and McMenamin, 2008). Interestingly, despite the extensive degeneration after light exposure, there were no signs of inflammation-induced disruption of the normal organization of the remaining retinal layers. Apparently conflicting results have been published on the role of retinal microglia in the degeneration of photoreceptor cells (Zhang et al., 2004, Hughes et al., 2004). Further research is warranted to elucidate the effects of microglial cells on photoreceptors.

ACKNOWLEDGMENTS

Thanks are due to Concepción Hernández for preparation of TEM samples, to David Porcel for TEM and confocal microscopy observations, and to Richard Davies for improving the English style of the manuscript.

LITERATURE CITED

Alarcón R, Fuenzalida C, Santibáñez M, von Bernhardi R. 2005. Expression of scavenger receptors in glial cells. Comparing the adhesion of astrocytes and microglia from neonatal rats to surface-bound beta-amyloid. J Biol Chem 280:30406–30415.

Ashwell KW, Hollander H, Streit W, Stone J. 1989. The appearance and distribution of microglia in the developing retina of the rat. Vis Neurosci 2:437–448.

Austyn JM, Gordon S. 1981. F4/80, a monoclonal antibody directed specifically against the mouse macrophage. Eur J Immunol 11:805–815.

Bell MD, Lopez-Gonzalez R, Lawson L, Hughes D, Fraser I, Gordon S, Perry VH. 1994. Upregulation of the macrophage scavenger receptor in response to different forms of injury in the CNS. J Neurocytol 23:605–613.

Biber K, Neumann H, Inoue K, Boddeke HW. 2007. Neuronal 'On' and 'Off' signals control microglia. Trends Neurosci 30:596–602.

Block ML, Hong JS. 2005. Microglia and inflammation-mediated neurodegeneration: multiple triggers with a common mechanism. Prog Neurobiol 76:77–98.

Block ML, Zecca L, Hong JS. 2007. Microglia-mediated neurotoxicity: uncovering the molecular mechanisms. Nat Rev Neurosci 8:57–69.

Chang GQ, Hao Y, Wong F. 1993. Apoptosis: final common pathway of photoreceptor death in rd, rds, and rhodopsin mutant mice. Neuron 11:595–605.

Chen L, Yang P, Kijlstra A. 2002. Distribution, markers, and functions of retinal microglia. Ocul Immunol Inflamm 10:27–39.

Cuadros MA, Navascues J. 1998. The origin and differentiation of microglial cells during development. Prog Neurobiol 56:173–189.

Cuadros MA, Santos AM, Martín-Oliva D, Calvente R, Tassi M, Marín-Teva JL, Navascués J. 2006. Specific immunolabeling of brain macrophages and microglial cells in developing and mature chick central nervous system. J Histochem Cytochem 54:727–738.

Da Silva RP, Gordon S. 1999. Phagocytosis stimulates alternative glycosylation of macrosialin (mouse CD68), a macrophage-specific endosomal protein. Biochem J 338:687–694.

Daugherty A, Whitman SC, Block AE, Rateri DL. 2000. Polymorphism of class A scavenger receptors in C57BL/6 mice. J Lipid Res 41:1568–1577.

Davalos D, Grutzendler J, Yang G, Kim JV, Zuo Y, Jung S, Littman DR, Dustin ML, Gan WB. 2005. ATP mediates rapid microglial response to local brain injury in vivo. Nat Neurosci 8:752–758.

Davies MH, Eubanks JP, Powers MR. 2006. Microglia and macrophages are increased in response to ischemia-induced retinopathy in the mouse retina. Mol Vis 12:467–477.

Diaz-Araya CM, Provis JM, Penfold PL, Billson FA. 1995. Development of microglial topography in human retina. J Comp Neurol 363:53–68.

Dissing-Olesen L, Ladeby R, Nielsen HH, Toft-Hansen H, Dalmau I, Finsen B. 2007. Axonal lesion-induced microglial proliferation and microglial cluster formation in the mouse. Neuroscience 149:112–122.

El Khoury J, Luster AD. 2008. Mechanisms of microglia accumulation in Alzheimer's disease: therapeutic implications. Trends Pharmacol Sci 29:626–632.

Fraser I, Hughes D, Gordon S. 1993. Divalent cation-independent macrophage adhesion inhibited by monoclonal antibody to murine scavenger receptor. Nature 364:343–346.

Garcia-Valenzuela E, Sharma SC, Pina AL. 2005. Multilayered retinal microglial response to optic nerve transection in rats. Mol Vis 11:225–231.

Gavrieli Y, Sherman Y, Ben-Sasson SA. 1992. Identification of programmed cell death in situ via specific labeling of nuclear DNA fragmentation. J Cell Biol 119:493–501.

Gowing G, Philips T, Van Wijmeersch B, Audet JN, Dewil M, Van Den Bosch L, Billiau AD, Robberecht W, Julien JP. 2008. Ablation of proliferating microglia does not affect motor neuron degeneration in amyotrophic lateral sclerosis caused by mutant superoxide dismutase. J Neurosci 28:10234–10244.

Grimm C, Wenzel A, Hafezi F, Remé CE. 2000. Gene expression in the mouse retina: the effect of damaging light. Mol Vis 6:252–260.

Gupta N, Brown KE, Milam AH. 2003. Activated microglia in human retinitis pigmentosa, late-onset retinal degeneration, and age-related macular degeneration. Exp Eye Res 76:463–471.

Hanisch UK, Kettenmann H. 2007. Microglia: active sensor and versatile effector cells in the normal and pathologic brain. Nat Neurosci 10:1387–1394.

Hao W, Wenzel A, Obin MS, Chen CK, Brill E, Krasnoperova NV, Eversole-Cire P, Kleyner Y, Taylor A, Simon MI, Grimm C, Remé CE, Lem J. 2002. Evidence for two apoptotic pathways in light-induced retinal degeneration. Nat Genet 32:254–260.

Harada T, Harada C, Kohsaka S, Wada E, Yoshida K, Ohno S, Mamada H, Tanaka K, Parada LF, Wada K. 2002. Microglia-Muller glia cell interactions control neurotrophic factor production during light-induced retinal degeneration. J Neurosci 22:9228–9236.

Herber DL, Maloney JL, Roth LM, Freeman MJ, Morgan D, Gordon MN. 2006. Diverse microglial responses after intrahippocampal administration of lipopolysaccharide. Glia 53:382–391.

Hughes EH, Schlichtenbrede FC, Murphy CC, Sarra GM, Luthert PJ, Ali RR, Dick AD. 2003. Generation of activated sialoadhesin-positive microglia during retinal degeneration. Invest Ophthalmol Vis Sci 44:2229–2234.

Hughes EH, Schlichtenbrede FC, Murphy CC, Broderick C, van Rooijen N, Ali RR, Dick AD. 2004. Minocycline delays photoreceptor death in the rds mouse through a microglia-independent mechanism. Exp Eye Res 78:1077–1084.

Hume DA, Gordon S. 1983. Mononuclear phagocyte system of the mouse defined by immunohistochemical localization of antigen F4/80. Identification of resident macrophages in renal medullary and cortical interstitium and the juxtaglomerular complex. J Exp Med 157:1704–1709.

Husemann J, Loike JD, Anankov R, Febbraio M, Silverstein SC. 2002. Scavenger receptors in neurobiology and neuropathology: their role on microglia and other cells of the nervous system. Glia 40:195–205.

Inman DM, Horner PJ. 2007. Reactive nonproliferative gliosis predominates in a chronic mouse model of glaucoma. Glia 55:942–953.

Joly S, Francke M, Ulbricht E, Beck S, Seeliger M, Hirrlinger P, Hirrlinger J, Lang KS, Zinkernagel M, Odermatt B, Samardzija M, Reichenbach A, Grimm C, Remé CE. 2009. Cooperative phagocytes: resident microglia and bone marrow immigrants remove dead photoreceptors in retinal lesions. Am J Pathol 174:2310–2323.

Keller C, Grimm C, Wenzel A, Hafezi F, Remé C. 2001. Protective effect of halothane anesthesia on retinal light damage: inhibition of metabolic rhodopsin regeneration. Invest Ophthalmol Vis Sci 42:476–480.

Kezic J, McMenamin PG. 2008. Differential turnover rates of monocyte-derived cells in varied ocular tissue microenvironments. J Leukoc Biol 84:721–729.

Kezic J, Xu H, Chinnery HR, Murphy CC, McMenamin PG. 2008. Retinal microglia and uveal tract dendritic cells and macrophages are not CX3CR1 dependent in their recruitment and distribution in the young mouse eye. Invest Ophthalmol Vis Sci 49:1599–1608.

Kreutzberg GW. 1996. Microglia: a sensor for pathological events in the CNS. Trends Neurosci 19:312–318.

Kunchithapautham K, Rohrer B. 2007. Apoptosis and autophagy in photoreceptors exposed to oxidative stress. Autophagy 3:433–441.

Kurushima H, Ramprasad M, Kondratenko N, Foster DM, Quehenberger O, Steinberg D. 2000. Surface expression and rapid internalization of macrosialin (mouse CD68) on elicited mouse peritoneal macrophages. J Leukoc Biol 67:104–108.

Lai AY, Todd KG. 2008. Differential regulation of trophic and proinflammatory microglial effectors is dependent on severity of neuronal injury. Glia 56:259–270.

Lalancette-Hébert M, Gowing G, Simard A, Weng YC, Kriz J. 2007. Selective ablation of proliferating microglial cells exacerbates ischemic injury in the brain. J Neurosci 27:2596–2605.

Langmann T. 2007. Microglia activation in retinal degeneration. J Leukoc Biol 81:1345–1351.

Lee JE, Liang KJ, Fariss RN, Wong WT. 2008. Ex vivo dynamic imaging of retinal microglia using time-lapse confocal microscopy. Invest Ophthalmol Vis Sci 49:4169–4176.

Lewis GP, Sethi CS, Carter KM, Charteris DG, Fisher SK. 2005. Microglial cell activation following retinal detachment: a comparison between species. Mol Vis 11:491–500.

Lohr HR, Kuntchithapautham K, Sharma AK, Rohrer B. 2006. Multiple, parallel cellular suicide mechanisms participate in photoreceptor cell death. Exp Eye Res 83:380–389.

Marella M, Chabry J. 2004. Neurons and astrocytes respond to prion infection by inducing microglia recruitment. J Neurosci 24:620–627.

Marin-Teva JL, Calvente R, Cuadros MA, Almendros A, Navascues J. 1999. Circumferential migration of ameboid microglia in the margin of the developing quail retina. Glia 27:226–238.

Mato M, Ookawara S, Sakamoto A, Aikawa E, Ogawa T, Mitsuhashi U, Masuzawa T, Suzuki H, Honda M, Yazaki Y, Watanabe E, Luoma J, Yla-Herttuala S, Fraser I, Gordon S, Kodama T. 1996. Involvement of specific macrophage-lineage cells surrounding arterioles in barrier and scavenger function in brain cortex. Proc Natl Acad Sci U S A 93:3269–3274.

McMenamin PG. 1999. Subretinal macrophages in the developing eye of eutherian mammals and marsupials. Anat Embryol (Berl) 200:551–558.

Ng TF, Streilein JW. 2001. Light-induced migration of retinal microglia into the subretinal space. Invest Ophthalmol Vis Sci 42:3301–3310.

Nimmerjahn A, Kirchhoff F, Helmchen F. 2005. Resting microglial cells are highly dynamic surveillants of brain parenchyma in vivo. Science 308:1314–1318.

Noell WK, Walker VS, Kang BS, Berman S. 1966. Retinal damage by light in rats. Invest Ophthalmol 5:450–473.

Pei Z, Pang H, Qian L, Yang S, Wang T, Zhang W, Wu X, Dallas S, Wilson B, Reece JM, Miller DS, Hong JS, Block ML. 2007. MAC1 mediates LPS-induced production of superoxide by mi-

croglia: the role of pattern recognition receptors in dopaminergic neurotoxicity. Glia 55:1362–1373.
Peiser L, Mukhopadhyay S, Gordon S. 2002. Scavenger receptors in innate immunity. Curr Opin Immunol 14:123–128.
Penninger JM, Irie-Sasaki J, Sasaki T, Oliveira-dos-Santos AJ. 2001. CD45: new jobs for an old acquaintance. Nat Immunol 2:389–396.
Perry VH, Hume DA, Gordon S. 1985. Immunohistochemical localization of macrophages and microglia in the adult and developing mouse brain. Neuroscience 15:313–326.
Pierce EA. 2001. Pathways to photoreceptor cell death in inherited retinal degenerations. Bioessays 23:605–618.
Platt N, Gordon S. 2001. Is the class A macrophage scavenger receptor (SR-A) multifunctional?—The mouse's tale. J Clin Invest 108:649–654.
Polazzi E, Contestabile A. 2002. Reciprocal interactions between microglia and neurons: from survival to neuropathology. Rev Neurosci 13:221–242.
Portera-Cailliau C, Sung CH, Nathans J, Adler R. 1994. Apoptotic photoreceptor cell death in mouse models of retinitis pigmentosa. Proc Natl Acad Sci U S A 91:974–978.
Provis JM, Diaz CM, Penfold PL. 1996. Microglia in human retina: a heterogeneous population with distinct ontogenies. Perspect Dev Neurobiol 3:213–222.
Raivich G, Bohatschek M, Kloss CU, Werner A, Jones LL, Kreutzberg GW. 1999. Neuroglial activation repertoire in the injured brain: graded response, molecular mechanisms and cues to physiological function. Brain Res Brain Res Rev 30:77–105.
Rao NA, Kimoto T, Zamir E, Giri R, Wang R, Ito S, Pararajasegaram G, Read RW, Wu GS. 2003. Pathogenic role of retinal microglia in experimental uveoretinitis. Invest Ophthalmol Vis Sci 44:22–31.
Remé CE, Grimm C, Hafezi F, Marti A, Wenzel A. 1998. Apoptotic cell death in retinal degenerations. Prog Retin Eye Res 17:443–464.
Remé CE, Grimm C, Hafezi F, Iseli HP, Wenzel A. 2003. Why study rod cell death in retinal degenerations and how? Doc Ophthalmol 106:25–29.
Rogove AD, Lu W, Tsirka SE. 2002. Microglial activation and recruitment, but not proliferation, suffice to mediate neurodegeneration. Cell Death Differ 9:801–806.
Roque RS, Imperial CJ, Caldwell RB. 1996. Microglial cells invade the outer retina as photoreceptors degenerate in Royal College of Surgeons rats. Invest Ophthalmol Vis Sci 37:196–203.
Sancho-Pelluz J, Arango-Gonzalez B, Kustermann S, Romero FJ, van Veen T, Zrenner E, Ekstrom P, Paquet-Durand F. 2008. Photoreceptor cell death mechanisms in inherited retinal degeneration. Mol Neurobiol 38:253–269.
Santos AM, Calvente R, Tassi M, Carrasco MC, Martin-Oliva D, Marin-Teva JL, Navascues J, Cuadros MA. 2008. Embryonic and postnatal development of microglial cells in the mouse retina. J Comp Neurol 506:224–239.
Sasahara M, Otani A, Oishi A, Kojima H, Yodoi Y, Kameda T, Nakamura H, Yoshimura N. 2008. Activation of bone marrow-derived microglia promotes photoreceptor survival in inherited retinal degeneration. Am J Pathol 172:1693–1703.
Solovjov DA, Pluskota E, Plow EF. 2005. Distinct roles for the alpha and beta subunits in the functions of integrin alphaMbeta2. J Biol Chem 280:1336–1345.
Tambuyzer BR, Ponsaerts P, Nouwen EJ. 2009. Microglia: gatekeepers of central nervous system immunology. J Leukoc Biol 85:352–370.
Thanos S. 1992. Sick photoreceptors attract activated microglia from the ganglion cell layer: a model to study the inflammatory cascades in rats with inherited retinal dystrophy. Brain Res 588:21–28.
Wakselman S, Bechade C, Roumier A, Bernard D, Triller A, Bessis A. 2008. Developmental neuronal death in hippocampus requires the microglial CD11b integrin and DAP12 immunoreceptor. J Neurosci 28:8138–8143.
Wenzel A, Grimm C, Samardzija M, Remé CE. 2005. Molecular mechanisms of light-induced photoreceptor apoptosis and neuroprotection for retinal degeneration. Prog Retin Eye Res 24:275–306.
Yamada Y, Doi T, Hamakubo T, Kodama T. 1998. Scavenger receptor family proteins: roles for atherosclerosis, host defence and disorders of the central nervous system. Cell Mol Life Sci 54:628–640.
Yamato S, Hirabayashi Y, Sugihara H. 1984. An improved procedure for the histochemical demonstration of cathepsin D by the mercury-labeled pepstatin method. Stain Technol 59:113–120.
Zeiss CJ, Johnson EA. 2004. Proliferation of microglia, but not photoreceptors, in the outer nuclear layer of the rd-1 mouse. Invest Ophthalmol Vis Sci 45:971–976.
Zeiss CJ, Neal J, Johnson EA. 2004. Caspase-3 in postnatal retinal development and degeneration. Invest Ophthalmol Vis Sci 45:964–970.
Zeng HY, Zhu XA, Zhang C, Yang LP, Wu LM, Tso MO. 2005. Identification of sequential events and factors associated with microglial activation, migration, and cytotoxicity in retinal degeneration in rd mice. Invest Ophthalmol Vis Sci 46:2992–2999.
Zhang C, Lei B, Lam TT, Yang F, Sinha D, Tso MO. 2004. Neuroprotection of photoreceptors by minocycline in light-induced retinal degeneration. Invest Ophthalmol Vis Sci 45:2753–2759.
Zhang C, Shen JK, Lam TT, Zeng HY, Chiang SK, Yang F, Tso MO. 2005. Activation of microglia and chemokines in light-induced retinal degeneration. Mol Vis 11:887–895.